

Quantum phase transitions in one-dimensional long Josephson junction stacks in parallel magnetic fields

Ju H. Kim

Department of Physics, University of North Dakota, P.O. Box 7129, Grand Forks, North Dakota 58202

(Received 5 November 2001; published 14 February 2002)

We report the effect of quantum and thermal fluctuations on stability of mutual phase locking in one-dimensional long Josephson junction devices, involving layered superconductors. Accounting for both the induction coupling and the charging effect, we determined the zero-temperature ($T=0$) phase diagram, using renormalization-group analysis, and found that the *in-phase* mode is stable, but some *out-of-phase* modes are unstable against quantum fluctuations. At finite T , all stable phase-locking modes (at $T=0$) are unstable, but stability is still maintained within a finite length, which decreases inversely with T . In $\text{Bi}_2\text{Sr}_2\text{CaCu}_2\text{O}_{8+y}$, this length for the *in-phase* mode is roughly $1000 \mu\text{m}$ at 1 K.

DOI: 10.1103/PhysRevB.65.100509

PACS number(s): 74.40.+k, 74.50.+r

Layered superconductors, such as $\text{YBa}_2\text{Cu}_3\text{O}_7$ and $\text{Bi}_2\text{Sr}_2\text{CaCu}_2\text{O}_{8+y}$ (BSCCO), are a strong candidate for terahertz oscillators because they have large superconducting energy gaps and behave as vertical stacks of long Josephson junctions (LJJ), as shown in Fig. 1. For device applications, high power output and bandwidth are desirable. These characteristics are obtained when stable mutual phase locking of Josephson junctions is maintained¹ in a magnetic field parallel to the S layers. Mutual phase locking, both *in-phase* and *out-of-phase* as shown in Fig. 2, is caused by (magnetic) inductive coupling between screening currents flowing around adjacent Josephson vortices (fluxons) as they move under a bias current. While all the phase-locked modes are obtained adjusting the bias current and the field strength, the *in-phase* mode is most useful. Consequently, stability of this mode is a focus of much interest.^{2,3} Recent numerical simulations of a stack of 20 LJJ (i.e., $N=20$), using one-dimensional (1D) sine-Gordon equations but neglecting the quantum and thermal fluctuation effects, indicate that the *in-phase* mode is stable against small external perturbations.³ However, the fluctuation effects are strong in one dimension. For example, quantum fluctuations yield the Kosterlitz-Thouless-Berezinskii- (KTB) type transition⁴ in the 1D Josephson-junction array (JJA) at zero temperature ($T=0$),⁵ indicating that these effects can destabilize the phase-locked mode. However, this mode instability was not investigated for a stack of 1D LJJ.

In this paper, we discuss the effect of quantum and thermal fluctuations on stability of the phase-locked mode in BSCCO. As suggested by earlier studies,⁶⁻⁸ we use a theoretical model for collective phase dynamics, which accounts for (i) the inductive coupling and (ii) the presence of a nonequilibrium state due to either the particle-hole imbalance⁸ or the breakdown of local charge neutrality⁷ (i.e., charging effect) because of the small S layer thickness, d_S ($\sim 3 \text{ \AA}$). Note that both the induction coupling and the effect of a nonequilibrium state are equally important for the phase dynamics, when d_S is comparable to the Debye (charge screening) length, r_D , which is at the atomic scale. Here we consider only the charging effect to account for the presence of a nonequilibrium state, as is usually done, because its strength⁷

$\alpha = \epsilon r_D^2 / \mathcal{D} d_S$ is more easily controlled. Since α depends inversely on the block layer thickness \mathcal{D} , α can be adjusted, intercalating the I layers with HgI_2 .⁹ Also, α is a nonthermodynamic parameter and regulates the amplitude of fluctuations at $T=0$, indicating that the 1D LJJ system can undergo the quantum phase transition (QPT).

Before proceeding further, we outline the main result of this work. We obtain the quantum phase diagram for a stack of 1D LJJ at $T=0$, using renormalization-group (RG) analysis, and find that the *in-phase* mode is stable, but the *out-of-phase* mode with a large wave number k_m in the z direction is unstable against quantum fluctuations. All stable phase-locked modes become unstable at finite T , but stability is maintained within a finite length scale (along the S layers) which decreases inversely with T . This length scale for the *in-phase* mode in BSCCO is roughly $1000 \mu\text{m}$ at 1 K.

To include both the magnetic induction coupling⁶ and the charging effect,⁷ we start with the coupled time-dependent sine-Gordon equations derived¹⁰ by Kim for a stack of 1D LJJ. Here we consider a system with a large number of LJJ

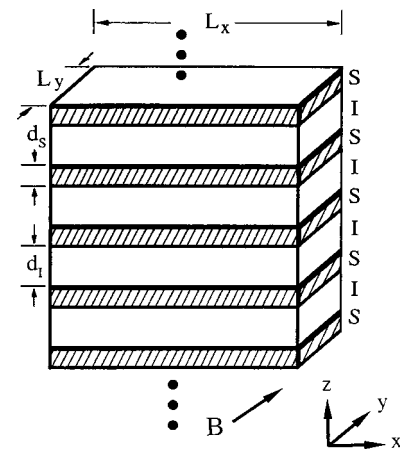


FIG. 1. Stack of LJJ is shown schematically as alternating superconducting (S) and insulating (I) layers with thicknesses d_S and d_I , respectively. L_x and L_y denote the dimensions in the x and y directions, respectively. The magnetic field is applied in the plane of tunnel barriers.

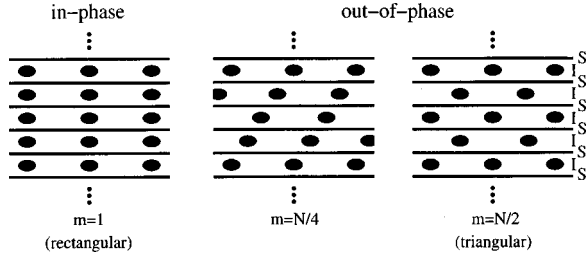


FIG. 2. Mutual phase locking of Josephson vortices (filled ovals) with the wave number $k_m = 2\pi m/(N+1)a$ in the z direction is schematically illustrated. Here, N is the number of LJJ in the stack and $a = d_S + d_I$. For the *in-phase* mode ($m=1$), the moving Josephson vortices form a rectangular lattice, but for the *out-of-phase* mode ($m=N/2$), they form a triangular lattice.

(i.e., $N \gg 1$) so that the boundary effect can be neglected. We set $\hbar = k_B = c = 1$. For convenience, we assume that the S and I layers with uniform thicknesses d_S and d_I , respectively, are stacked in the z direction and the magnetic field is applied in the y direction, as shown in Fig. 1. Since the dissipation (β) and charging effects (α) are small in BSCCO ($\alpha \sim 0.1$ and $\beta \sim 0.2$),¹¹ the collective phase dynamics of the gauge-invariant phase difference $\varphi_{l,l-1}$ between the l th and $(l-1)$ th S layers, under a finite bias current, is described¹⁰ by

$$\begin{aligned} & \frac{\partial^2 \varphi_{l,l-1}}{\partial x^2} - \frac{1}{\lambda_c^2 \mathcal{D}} \left(\frac{1}{\omega_p^2} \frac{\partial^2}{\partial t^2} + \frac{\beta}{\omega_p} \frac{\partial}{\partial t} \right) \\ & \times [d' \varphi_{l,l-1} + s(\varphi_{l+1,l} + \varphi_{l-1,l-2})] \\ & - \frac{\alpha}{\lambda_c^2 \mathcal{D}} \frac{1}{\omega_p^2} \left(\frac{\partial^2 \Xi_l}{\partial t^2} \right) \\ & = \frac{1}{\lambda_c^2 \mathcal{D}} [d' \sin \varphi_{l,l-1} + s(\sin \varphi_{l+1,l} + \sin \varphi_{l-1,l-2})], \end{aligned} \quad (1)$$

neglecting the higher-order terms, such as $\mathcal{O}(\alpha\beta)$ and $\mathcal{O}(\alpha^2)$. The term $\Xi_l = s(\varphi_{l-2,l-3} + \varphi_{l+2,l+1}) + (d' - 2s)(\varphi_{l-1,l-2} + \varphi_{l+1,l}) + 2(s - d')\varphi_{l,l-1}$ accounts for the coupling between the S layers due to the charging effect. $\omega_p = 1/\sqrt{\epsilon\lambda_c}$ is the plasma frequency, ϵ is the dielectric constant in the I layers, $\lambda_c = (16e\pi^2 \mathcal{D} J_c)^{-1/2}$, J_c is the Josephson current, $\mathcal{D} = d' + 2s$, $d' = d_I + 2\lambda \coth(d_S/\lambda)$, and $s = -\lambda[\sinh(d_S/\lambda)]^{-1}$. When the charging effect is absent ($\alpha = 0$), Eq. (1) recovers the sine-Gordon equations for a multilayer system, derived by Bulaevskii *et al.*¹² To capture the 1D nature of collective phase dynamics of Eq. (1), the physical devices must be short in the y direction (i.e., L_y). For simplicity, we neglect the dissipation effect (i.e., $\beta = 0$) in the discussion below.

The dynamics of the sine-Gordon Eq. (1) is described using a Lagrangian. In BSCCO, the Lagrangian \mathcal{L} corresponding to Eq. (1) is found, taking advantage of the fact that the induction coupling is close to the strong-coupling limit. Note that $S = s/d' = -0.49999$ for BSCCO (since $\lambda \sim 1500$, $d_I \sim 15$, and $d_S \sim 3 \text{ \AA}$), while $S = -0.5$ in the strong-

coupling limit. Noting that $1 + 2S \ll 1$ and introducing the gauge-invariant phase¹³ ψ_l for the l th layer (i.e., $\varphi_{l,l-1} = \psi_l - \psi_{l-1}$), we reduce Eq. (1) to

$$\begin{aligned} & \Lambda_c^2 \frac{\partial^2 \psi_l}{\partial x^2} - \frac{1}{\omega_p^2} \frac{\partial^2}{\partial t^2} [-\omega_{l+1} + 2\psi_l - \psi_{l-1} \\ & - \alpha(\psi_{l+2} - 4\psi_{l+1} + 6\psi_l - 4\psi_{l-1} + \psi_{l-2})] \\ & = -\sin(\psi_{l+1} - \psi_l) + \sin(\psi_l - \psi_{l-1}). \end{aligned} \quad (2)$$

Here $\Lambda_c^2 = -\lambda_c^2 \mathcal{D}/d'S$. For convenience, we introduce the dimensionless *spacelike* and *timelike* coordinates by making the transformations $x/\Lambda_c \rightarrow x$ and $\omega_p t \rightarrow t$. One can now see easily that the dynamics of ψ_l , described by Eq. (2), is obtained from

$$\begin{aligned} \mathcal{L} = \sum_l & \left\{ \frac{1}{2} \left[\left(\frac{\partial \psi_l}{\partial x} \right)^2 + \left(\frac{\partial [\psi_l - \psi_{l-1}]}{\partial \tau} \right)^2 \right. \right. \\ & \left. \left. - \alpha \left(\frac{\partial [\Delta^{(2)} \psi_l]}{\partial \tau} \right)^2 \right] + [1 - \cos(\psi_l - \psi_{l-1})] \right\}, \end{aligned} \quad (3)$$

where $\Delta^{(2)} \psi_l = (\psi_l - \psi_{l-1}) - (\psi_{l-1} - \psi_{l-2})$ and $\tau = it$ denotes the imaginary timelike coordinate. The effects of quantum and thermal fluctuations on stability of phase locking are determined using the partition function $\mathcal{Z} = \int \mathcal{D}\psi_l e^{-S[\psi_l]}$, where $S[\psi_l] = \int_0^{1/T} d\tau \int dx \mathcal{L}$. In the remainder of the paper, we discuss the fluctuation effects (both for $T=0$ and $\neq 0$) on the phase dynamics, using the Lagrangian (3) in the functional integral \mathcal{Z} .

First, we discuss the effect of quantum fluctuations. At $T=0$, the phase-coherence time τ_φ , the time scale for retaining the memory of its phase, is infinite (i.e., $\tau_\varphi = \infty$), and hence, τ_φ does not play a role. Note τ_φ is defined, writing the correlation function $\Gamma(x, t)$, which we will discuss below, in terms of a reduced scaling function $\Phi_R(x, t)$ as $\Gamma(0, t) \propto \Phi_R(0, t) \sim e^{-t/\tau_\varphi}$.¹⁴ Since the system size in the τ direction diverges as $T \rightarrow 0$, the 1D LJJ stack is described using (1+1)D classic statistical mechanics. Noting that the sine-Gordon model of Eq. (3) is mapped onto the 2D neutral Coulomb gas model (or the 2D XY model) in $\mathbf{r} = (x, \tau)$,¹⁵ we reduce \mathcal{Z} to a familiar form in the following four steps: first, write ψ_l as Fourier series $\psi_l = \sum_{k_m} \psi_{k_m} e^{-ik_m a l}$; second, go back to the phase difference representation $\varphi_{l,l-1} = \sum_{k_m} \varphi_{k_m} e^{-ik_m a l}$ [i.e., $\varphi_{k_m} = (1 - e^{-ik_m a}) \psi_{k_m}$]; third, integrate out φ_{k_m} ; and finally, rescale the coordinates to $\bar{\mathbf{r}} = (x K_m^x, \tau/K_m^\tau) = (\bar{x}, \bar{\tau})$. We write the partition function as $\mathcal{Z} = \mathcal{C} \prod_{k_m} \mathcal{Z}_{k_m}$, where the phase-locked mode contribution¹⁶ \mathcal{Z}_{k_m} is

$$\begin{aligned} \mathcal{Z}_{k_m} = & \sum_{n_{k_m}} \frac{z^{2n_{k_m}}}{(n_{k_m}!)^2} \int \frac{d^2 \bar{\mathbf{r}}_1}{\xi_c^2} \cdots \int \frac{d^2 \bar{\mathbf{r}}_{2n_{k_m}}}{\xi_c^2} \\ & \times \exp \left(2\pi K_m \sum_{j \neq l} q_{j,k_m} q_{l,-k_m} \ln \frac{|\bar{\mathbf{r}}_j - \bar{\mathbf{r}}_l|}{\xi_c} \right), \end{aligned} \quad (4)$$

$C = \exp[1/2 \sum_{k_m} (K_m T / \omega_p) \sum_{\omega_n} \int (dk/2\pi) \ln(k^2 + \omega_n^2)]$, $K_m^x = (K_m^\tau / K_m^c)^{1/2}$ is the effective coupling constant, $K_m^x = 2(1 - \cos k_m a)$, $K_m^\tau = 1 - 2\alpha(1 - \cos k_m a)$, $k_m = 2\pi m / (N+1)$ (with $m = 1, 2, \dots, N$), $\omega_n = (2n\pi T) K_m^\tau / \omega_p$, n_{k_m} is the number of positively (and negatively) charged particles, q_j is the charge located at $\bar{\mathbf{r}}_j$, ξ_c is the distance between the charges, and $z = K_m e^{-\pi^2 K_m^2}$ is the fugacity. Note that decoupling¹⁶ of the phase-locked modes allows one to examine the stability of each mode separately. Z_{k_m} of Eq. (4) is similar to that for the 2D Coulomb gas model,¹⁷ but there are two important differences: (i) K_m does not depend on T but (ii) it does depend on both k_m and α . Hence the LJJ stack exhibits QPT as k_m and α change. This QPT is identical to the KTB transition between the (low- T) ordered phase and the (high- T) disordered phase in the 2D classical XY model.

The ordered and disordered phases of Eq. (4) represent the *stable* and *unstable* regions for the phase-locked mode, respectively, since the appearance of unbound charges in the Coulomb gas model corresponds to the quantum phase slip in 1D LJJ, as in the 1D JJA, due to the fluxon-antifluxon disassociation. The *stable-unstable* phase boundary at $T=0$ is determined using RG analysis.¹⁸ Scaling of the charge separation distance from ξ_c to $\xi_c + d\xi_c$ (to the lowest order in fugacity) yields

$$\frac{dx}{d\xi_c} = -\frac{y^2}{\xi_c}, \quad (5)$$

$$\frac{dy}{d\xi_c} = -\frac{xy}{\xi_c}, \quad (6)$$

where $x = Q^2 - 2$, $y = 4\pi\bar{K}\xi_c^2$, $Q^2 = \pi K_m q_{k_m} q_{-k_m}$, and $\bar{K}\xi_c^2 = K_m e^{-\pi^2 K_m^2}$. These scaling equations indicate that the RG flow trajectories lie along $x^2 - y^2 = \text{const}$ and flow to the stable critical fixed line $y=0$ for $K_m > K_m^c$. Along $y=0$, the quantum sine-Gordon model of Eq. (3) corresponds exactly to a free-field model. Hence, the *stable* and *unstable* phases from Eqs. (5) and (6), characterized by the correlation function $\Gamma(\bar{r}) = \langle e^{i\varphi(\bar{r})} e^{-i\varphi(0)} \rangle$,

$$\Gamma(\bar{r}) \sim \begin{cases} \frac{1}{\bar{r}^{\eta(K_m)}} & \text{for } K_m > K_m^c, \\ e^{-\bar{r}/\xi} & \text{for } K_m < K_m^c, \end{cases} \quad (7)$$

where $\bar{r} = (\bar{x}^2 + \bar{r}^2)^{1/2}$, indicate that the correlation length ξ is infinite (i.e., $\xi = \infty$) for $K_m > K_m^c$ (stable) but varies as $\xi \sim e^{A/[k_m^{-1} - (K_m^c)^{-1}]^{1/2}}$ for $K_m < K_m^c$ (unstable).¹⁸ Here the critical coupling constant K_m^c is determined from $\pi K_m^c - 2 = 4\pi K_m^c e^{-\pi^2 K_m^c}$. A simple numerical calculation reveals that $K_m^c \approx 0.7193$. The critical exponent $\eta(K_m) = \frac{1}{4}$ for $K_m = K_m^c$ but it is less than $\frac{1}{4}$ for $K_m > K_m^c$. The phase diagram for stability, shown in Fig. 3, indicates that the *in-phase* mode (the $m=1$ mode in Fig. 2) is stable, but the *out-of-phase* modes with large k_m (i.e., the $m=N/4$ and $N/2$ modes in Fig. 2) are unstable against quantum fluctuations. The phase boundary is shifted to a smaller k_m with increasing α

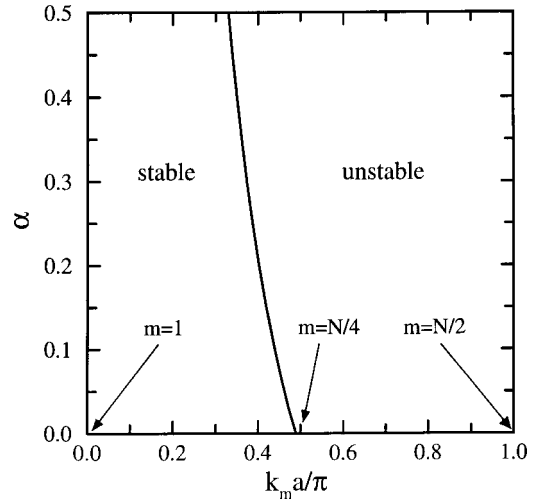


FIG. 3. The phase diagram for stability of the phase-locked mode at $T=0$, obtained from RG analysis.

since the charging effect enhances quantum fluctuations, but the *in-phase* mode (i.e., the $m=1$ mode in Fig. 2) remains stable.

We now discuss the effect of thermal fluctuations. At finite T , all phase-locked modes in the LJJ system are unstable since the temperature sets the system size to be finite in the τ direction (i.e., $L_\tau = 1/T$). The 1D systems have no long-range order at finite T . However, stability is still maintained within the time scale τ_φ . Note τ_φ is finite when T is nonzero. Near the quantum critical point (QCP) (i.e., $K_m = K_m^c$), the size of τ_φ (relative to L_τ) is used to separate the finite T phase diagram into the thermally disordered (TD), the quantum critical (QC), and the quantum disordered (QD) regimes, shown schematically in Fig. 4. First, in the TD region, thermal fluctuations are dominant, and ξ for $K_m > K_m^c$ is finite. Second, in the QC region, both thermal and quantum fluctuations are equally important. The dotted line separates the TD and QC regions, but the phase dynamics, in these two regions, are identical since $\tau_\varphi \geq L_\tau$. Finally, in the QD region, quantum fluctuations, rather than thermal fluctuations, destabilize the phase-locked mode since τ_φ is exponentially long (i.e., $\tau_\varphi \gg L_\tau$).¹⁴ This region is characterized by the con-

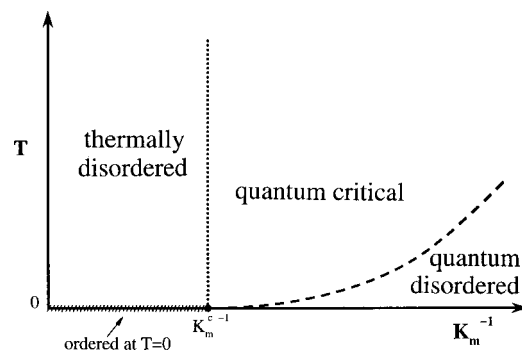


FIG. 4. The finite T phase diagram for the 1D LJJ stack system is shown schematically. The dotted line separates the TD region from the QC region, while the dashed line ($T \sim \Delta$) separates the QC region from the QD region.

dition $T \ll \Delta \sim e^{-A/[K_m^{-1} - (K_m^c)^{-1}]^{1/2}}$. The dashed line, representing $T \sim \Delta$, separates the QC region from the QD region.

We estimate the length scale $l_{m,\varphi}$ for maintaining stability (along the S layers) in the TD and the QC regions, computing τ_φ . The phase-coherence time $\tau_\varphi^{\text{TD QC}}$ in these regions is characterized by relaxational dynamics. We compute $\tau_\varphi^{\text{TD QC}}$, noting that the 1D LLJ system is scale invariant at the QCP and is described by free Gaussian theory, which is conformally invariant, for $K_m > K_m^c$. The conformal symmetry¹⁹ is used to compute the correlation function $\Gamma_{k_m}(\bar{x}, \bar{\tau}) = \langle e^{i\varphi_{k_m}(\bar{x}, \bar{\tau})} e^{-i\varphi_{k_m}(0,0)} \rangle$ at finite T from the result $\Gamma_{k_m}(\bar{r}) = [(\bar{\tau} + i\bar{x})(\bar{\tau} - i\bar{x})]^{\eta(K_m)/2}$ at $T=0$. Using the map $\bar{\tau} \pm i\bar{x} \rightarrow (\omega_p / \pi K_m^\tau T) \sin[(\pi K_m^\tau T / \omega_p)(\bar{\tau} \pm i\bar{x})]$, we write the two-point correlation function at finite T as

$$\Gamma_{k_m}(\bar{r}) \sim \left[\frac{(\pi K_m^\tau T / \omega_p)^2}{\sin \frac{\pi K_m^\tau T}{\omega_p} (\bar{\tau} + i\bar{x}) \sin \frac{\pi K_m^\tau T}{\omega_p} (\bar{\tau} - i\bar{x})} \right]^{\eta/2}. \quad (8)$$

The time scale for the relaxation dynamics is computed using the relation $\tau_{m,R} = i\chi_{k_m}(0,0)[\partial\chi_{k_m}^{-1}(0,\omega)/\partial\omega]_{\omega=0}$. The dynamical susceptibility $\chi_{k_m}(k,\omega)$ is obtained from analytical continuation of $i\omega_n$ in $\chi_{k_m}(k,i\omega_n) = \int_0^{\omega_p/T} d\tau \int dx e^{-i(kx - \omega_n\tau)} \Gamma_{k_m}(\bar{x}, \bar{\tau})$ to real frequencies (i.e., $i\omega_n \rightarrow \omega + i\delta$). Following the usual procedure²⁰ for evaluating the integrals in $\chi_{k_m}(k,i\omega_n)$, we obtain

$$\tau_{m,\varphi}^{\text{TD QC}} = \frac{1}{2T} \cot \frac{\pi\eta(K_m)}{4}, \quad (9)$$

indicating that the phase coherence is maximally incoherent. Hence, the length scale $l_{m,\varphi} = \bar{c}_m \tau_{m,\varphi}^{\text{TD QC}}$ decreases inversely with T . Here the Swihart velocity \bar{c}_m for the mode m ,¹⁰

$$\bar{c}_m = \frac{1}{\sqrt{\epsilon}} \left[\frac{1 + 4\alpha \sin^2 \frac{k_m a}{2}}{1 + 4 \left(\frac{-S}{1+2S} \right) \sin^2 \frac{k_m a}{2}} \right]^{1/2}, \quad (10)$$

represents the maximum speed for the moving phase-locked Josephson vortices. In BSCCO, assuming $\epsilon \approx 25$,¹¹ this length scale for the *in-phase* mode ($m=1$) and the *out-of-phase* mode (with $m=N/8$) modes at 1 K are roughly 1000 and 20 μm , respectively. This large value of $l_{m,\varphi}$ for the *in-phase* mode is due to the strong inductive coupling (i.e., $S = -0.49999$), which strongly enhances the Swihart velocity for $m=1$.^{1,10}

In summary, we investigated the effect of fluctuations on stability of the phase-locked mode in a stack of 1D LJJ. Our result shows that the nature of QPT in this system is the *stable-unstable* transition for the phase-locked mode, indicating the *out-of-phase* modes with large k_m are unstable but the *in-phase* mode is stable against quantum fluctuations. All phase-locked modes are found unstable at finite T , but stability is still maintained within the length $l_{m,\varphi}$, which decreases inversely with T . $l_{m,\varphi}$ for the *in-phase* mode in $\text{Bi}_2\text{Sr}_2\text{CaCu}_2\text{O}_{8+y}$ ($\sim 1000 \mu\text{m}$) is much larger than that for the *out-of-phase* mode due to strong inductive coupling. This work provides insight on the operating range of temperatures and the physical dimensions of LJJ devices for high power output applications requiring the stable *in-phase* mode. This prediction can be verified in the LJJ stack that is short (L_y) in the y direction since such devices are within reach of present day fabrication technology.

The author thanks KIAS, where a part of this work was completed. This work was supported in part by the UND Research Seed Money Program.

¹A. V. Ustinov and S. Sakai, Appl. Phys. Lett. **73**, 683 (1998); J. U. Lee *et al.*, *ibid.* **71**, 1412 (1997); N. F. Pedersen and S. Sakai, Physica C **332**, 297 (2000).
²A. E. Koshelev and I. S. Aranson, Phys. Rev. Lett. **85**, 3938 (2000); R. Kleiner *et al.*, Phys. Rev. B **62**, 4086 (2000); Physica C **362**, 29 (2001); R. Kleiner, Phys. Rev. B **50**, 6919 (1994).
³M. Machida *et al.*, Physica C **330**, 85 (2000).
⁴J. M. Kosterlitz and D. J. Thouless, J. Phys. C **6**, 1181 (1973); V. L. Berezinskii, Zh. Eksp. Teor. Fiz. **61**, 1144 (1971) [Sov. Phys. JETP **34**, 610 (1971)].
⁵See, for example, M. Y. Choi *et al.*, Phys. Rev. B **63**, 094516 (2001); R. M. Bradley and S. Doniach, *ibid.* **30**, 1138 (1984).
⁶S. Sakai *et al.*, J. Appl. Phys. **73**, 2411 (1993).
⁷M. Machida *et al.*, Phys. Rev. Lett. **83**, 4618 (1999), and references therein.
⁸S. N. Artemenko and A. G. Kobelkov, Phys. Rev. Lett. **78**, 3551 (1997); D. Ryndyk, *ibid.* **80**, 3376 (1998).
⁹Y.-J. Doh *et al.*, Phys. Rev. B **63**, 144523 (2001).
¹⁰J. H. Kim, Int. J. Mod. Phys. B **15**, 3347 (2001).

¹¹K. Schlenga *et al.*, Phys. Rev. B **57**, 14 518 (1998); Ch. Preis *et al.*, in *Superconducting Superlattices II*, SPIE Conference Proceedings (SPIE, Bellingham, WA, 1998), p. 236.
¹²L. N. Bulaevskii *et al.*, Phys. Rev. B **50**, 12 831 (1994).
¹³L. N. Bulaevskii and J. R. Clem, Phys. Rev. B **44**, 10 234 (1991).
¹⁴S. Sachdev, *Quantum Phase Transitions* (Cambridge University, Cambridge, England, 1999); S. L. Sondhi *et al.*, Rev. Mod. Phys. **69**, 315 (1997).
¹⁵P. M. Chaikin and T. C. Lubensky, *Principles of Condensed Matter Physics* (Cambridge University, New York, 1995).
¹⁶A similar mode decoupling was also found in an elastic theory for the stripe phase of the 2D electron gas in high Landau levels [see H. Yi, H. Fertig, and R. Côté, Phys. Rev. Lett. **85**, 4156 (2000)].
¹⁷P. Minnhagen, Rev. Mod. Phys. **59**, 1001 (1987).
¹⁸J. M. Kosterlitz, J. Phys. C **7**, 1046 (1974).
¹⁹J. L. Cardy, J. Phys. A **17**, L385 (1984).
²⁰H. J. Schultz, Phys. Rev. B **34**, 6372 (1986); S. Sachdev *et al.*, *ibid.* **50**, 258 (1994).